2011 50th IEEE Conference on Decision and Control and
European Control Conference (CDC-ECC)
Orlando, FL, USA, December 12-15, 2011

Sensors Searching for Interesting Things: Extremum Seeking Control on Entropy Maps

Yinghua Zhang, Mario Rotea and Nicholas Gans

Abstract— **This paper presents a novel approach to increasing the information content in sensor measurements, with special applications in images or video. The entropy of a signal gives a measurement of the information content. In the case of images, entropy is low when large parts of an image are uniformly colored or shaded. This can occur due to poor camera settings, poor lighting conditions, or the camera is facing a scene with little interest or activity. Minor camera motions can often alleviate these problems. We employ methods of extremum seeking control to find a local maximum in the entropy map surrounding the camera. Entropy maps often have local maxima that do not correspond to a global maximum. Therefore we combine the global properties of simplex optimization methods with the local search properties and dynamic response of extremum seeking control to create a novel algorithm that is more likely to find a global maximum than conventional extremum seeking control. Simulations and experiments are presented to show the strength of this approach.**

I. INTRODUCTION

Given limited sensors covering a wide area, a sensor needs to isolate targets of interest to maximize the value of its measurements. Alternately, given abundant sensors, the amount of data may overwhelm communication channels, processor bandwidth, or human observers, necessitating the ability to transmit only the most useful data. This paper presents an initial investigation to control the position of a sensor to collect the most valuable measurements via extremum seeking control (ESC) of sensor configuration. In particular, we seek to maximize the information content of image or video data to provide the most useful images.

ESC seeks to optimize the value of a measurable cost function [1]. The strength of this method is that no a priori knowledge of the cost function is necessary. A stability proof of ESC was first provided by Krstic and Wang for a general nonlinear SISO system [2]. Multivariable ESC was later studied by Rotea, and a set of detailed design guidelines for ESC were provided [3]. Recently, global ESC methods were studied by Tan and Nesic [4].

In casting optimization as a control problem to be optimized, the measured output of ESC is the cost function, while the control input is the vector of optimization variables. ESC attempts to optimize the measured cost function by adjusting the control inputs according to a gradient descent algorithm implemented in real time. The gradient is estimated by using an external, periodic perturbation (or dither signal) and a series of filtering and modulation operations. The estimated gradient is integrated to produce the control inputs, which constitute an estimate of the optimal set of variables. If the ESC loop is stable, then the inputs to the integrators will vanish when the system reaches steady state. This results in a zero gradient, which is a necessary condition for unconstrained optimization. Thus, in steady state, the system is at a local extremum point.

One measure of information contained in a signal is the signal entropy [5]. Shannon's entropy measure of information has found wide spread use in information and communication theory, as it provides a limit to lossless compression [6]. Entropy also has applications in estimation theory [7], [8].

We posit that maximum entropy can indicate an information rich data set. A DC signal will have zero entropy, while a uniformly distributed signal will have maximum entropy. In the context of images or video, a blank image, such as a camera facing a wall, will have lower entropy than an image of a busy environment. Using ESC to guide a sensor to the location of maximum entropy is an ideal approach, as knowledge of the entropy as a function of the sensor workspace is not needed. As the ESC guides the sensor to a point providing a signal of maximum entropy, we expect the signal to have more information.

Entropy has been used in sensor placement in previous research. Beni and Hackwood proposed that maximizing entropy with a swarm of sensors would maximize the probability that a single event would be detected [9]. Similarly, Abidi suggested using maximum expected entropy to choose the camera view of an object that adds the most new information [10]. These methods differ from the proposed approach in that they utilized offline optimization methods and knowledge of the scene and environment. The method proposed in this paper runs in real time, can adapt to dynamic environments, and does not require knowledge of the scene or environment.

Alternative approaches to sensor placement, and camera placement in particular, have been investigated. Several groups (e.g. Howard et al. [11], Murray et al [12], and Zou and Chakrabarty [13]) focused on coverage, i.e. maximizing the amount of area that is covered by at least one sensor. Mittal and Davis worked on placing sensors to avoid occlusions by static and moving objects [14]. Research by Zhao et al. focused on arranging multiple sensors to simultaneously measure areas or track targets [15]. Papanikolopoulos has investigated sensor placement to reduce the amount of processing that must be performed [16] or reducing the expected error in the final estimation [17]. Similar work was done by Ercan et al. [18]. Basar and his group has focused on

Y. Zhang and N. Gans are with the Department of Electrical Engineering, M. Rotea is with the Department of Mechanical Engineering, University of Texas at Dallas, Richardson, TX 75080, USA {yxz102220, rotea, ngans}@utdallas.edu

978-1-61284-799-3/11/$26.00 ©2011 IEEE

an optimal transmission policy, in which an observer of a stochastic process sends data to a remote estimator only if it will change the current estimate more than some threshold [19].

A contribution of this paper is a method to maximize the information content of signals (particularly images) in real time with no knowledge of the environment. This environment may be dynamic, meaning the entropy map is time varying. The proposed method will provide a general framework to select among sensors, place sensors, or control movable sensors to improve estimation accuracy and reduce transmission bandwidth. ESC methods have been developed for over a decade, and sufficient conditions for stability have been well established. This paper investigates the environmental conditions that allow for stable ESC of image entropy. We also investigate the choice of ESC design parameters, such as frequency of the differ signal, necessary for stability and performance given the slow sampling rate of most cameras (approximately 30Hz).

We also propose a new extremum seeking method that combines the dynamic properties of conventional ESC with the global convergence properties of simplex optimization algorithms [20]–[22]. This will increase the likelihood that the system converges to a global maximum. Additionally, it will ideally eliminate iterations of the simplex algorithm. We refer to this method as Simplex Guided Extremum Seeking (SGES). Simulations and experiments are performed to demonstrate the proposed methods.

II. Background

A. Extremum Seeking Control

ESC is designed to optimize a cost function in real time, without any prior knowledge of the input-to-cost mapping. References [2]–[4] concentrated on developing ESC methods. Fig. 1 shows a common scheme of ESC. The current estimate of the optimal state of the system is $\overline{\theta}(t) \in \mathbb{R}^n$. A dither signal $d_1(t) \in \mathbb{R}^n$ is added to $\overline{\theta}(t)$ to give the current state $\theta(t)$. The signal $d_1(t)$ is typically given by a vector of sinusoids $a_i \sin(\omega_i t), i = 1 \dots n$.

The output $y(t) \in \mathbb{R}$ can be expressed by the Taylor Series

$$y(t) = f(t,\bar{\theta}) + d_1(t)^T \frac{\partial f(t,\bar{\theta})}{\partial \theta} + H.O.T. \qquad (1)$$

Neglecting higher order terms, passing $y(t)$ through a high pass filter block gives a signal correlated to the gradient vector $\partial f(t,\bar{\theta})/\partial\theta$. The gradient is extracted via a demodulation scheme that multiplies the output of the high-pass filter by the dither signal $d_2(t) \in \mathbb{R}^n$, followed by application of a low-pass filter. The resulting signal $\zeta(t) \in \mathbb{R}^n$ is an estimate of the gradient. A signed scalar gain term k determines the direction and speed of motion (i.e. whether we seek maximum or minimum and the rate of convergence). Integrating $k\xi$ gives the current estimate of the optimal state $\overline{\theta}(t) \in \mathbb{R}^n$.

ESC systems are generally nonlinear. However, when the dither signal frequencies ω_i are large enough, averaging theory [23], [24] can provide a linear system that approximates

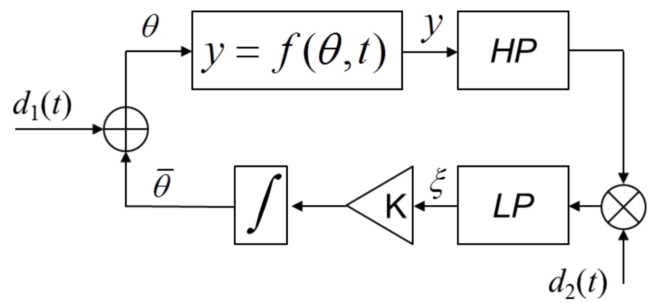

Fig. 1. Block Diagram of the Extremum Seeking Loop

the dynamics of the ESC loop. Using this linear approximation, reference [3] provides guidelines for selecting dither signals and filters to ensure closed loop stability of the ESC loop. In Section III-B we use these guidelines to design an ESC system for entropy maximization.

B. Entropy

Shannon's seminal work on communication defined the entropy H of a discrete random variable X as

$$H(X) = -\sum_{x\in X} p(x)\log(x) \qquad (2)$$

where $p(x)$ is the probability mass function giving the probability that $X = x$ [5], [25]. The entropy gives a measurement of the uncertainty associated with X. $H(X)$ takes its maximum when the random variable is uniformly distributed, in which case any particular x is equally likely. Likewise, $H(X)$ takes its minimum when the value x is completely determined, corresponding to $p(x) = \delta(x_0)$, where $\delta(x_0)$ is an impulse function at (x_0). In this case, there is no uncertainty in X. Shannon's entropy measure of information has found wide spread use in information and communication theory, as it provides a limit to lossless compression [6]. Entropy also has applications in estimation theory. The maximum entropy has been used to choose between distribution functions to find one that best fit the true distribution [7], [8]. In the context of real-time digital signal analysis, $p(X)$ is given by the histogram of the measured signal values. A DC signal will have zero entropy. A signal with a wide distribution band will have high entropy. In case of images, the variable X is the value of a pixel, and $p(X)$ is the histogram of pixel values in the image.

In the case of images, an image that is a single shade or color is a DC image and has zero entropy. An image with many shades and colors has high entropy. Examples of similar images with different entropy levels are seen in Fig. 2. There are several issue to consider with image entropy. One is the issue of color spaces. In a color image, each pixel has three color channel values. The image could be converted to gray scale and the entropy of the resulting intensity image can be calculated. However, information is lost when color images are converted to grayscale, studies have shown that color contributes heavily to interest in the human visual system. An alternative is to estimate entropy separately across each color channel and calculate an overall entropy as the sum or norm of all channels (a similar

Fig. 2. The two images on the left have lower entropy than the images on the right. This is caused by exposure or lighting conditions causing the left images to have large regions that are similarly colored or shaded. Specifically the upper left image has $H = 5.3$, while the upper right image has $H = 7.5$. The lower left image has $H = 7.2$ while the lower right image has $H = 7.7$.

approach was followed in [26]). Alternately, a 3D color histogram can be used. There may also be effects from using different color channels parameterizations (e.g. red-green-blue vs. hue-saturation-value). These issues will be explored in future research.

III. ESC Design for Entropy Maximization

In this Section, we provide the design parameters of the ESC loop to steer a camera to maximize the entropy of captured images. In this initial investigation, robot/camera motion is limited to a 2D vertical/horizontal plane, i.e. a 2D subspace of its 6DOF workspace, corresponding to the camera image plane. Entropy is maximized by adjusting the horizontal and vertical position of the camera. That is, the optimization variables are

$$\theta = [x, y]^T$$

where x and y are the coordinates of the camera in a plane perpendicular to the ground.

A. Entropy Mappings

ESC is an approach for unconstrained optimization. Hence, a necessary condition for stability or convergence is that the entropy map must posses a relative maximum in interior of the camera workspace. To test this condition, we conducted several experiments to build entropy mappings as a function of camera position. The experiments were conducted using a Staubli TX90 robot, with 6 degree of freedom. A camera is mounted on the end effector, and the offset from the camera to the end effector is previously calibrated. The robot can accept a commanded velocity or position of the camera, and motion was limited to a 2D plane.

We designed two experiments to represent common situations where maximizing the entropy would be useful. In the first experiment, a monochrome poster board was placed in front of the robot with a picture taped in the center. This represents a single area of interest in a largely uninteresting field. The entropy, as a function of the camera position $[x, y]^T$ is shown in Fig. 3. It clearly has global maximum in the interior of the workspace.

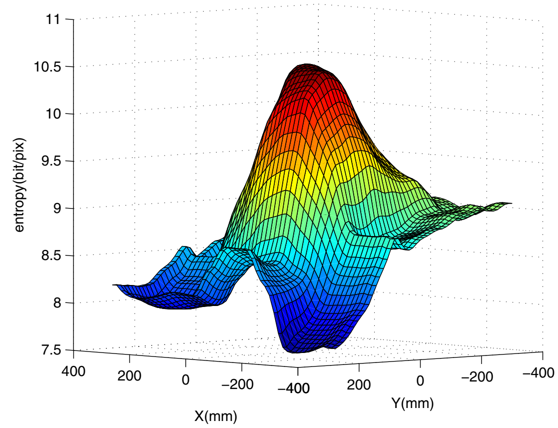

Fig. 3. Entropy Mapping with a Dominate Maximum

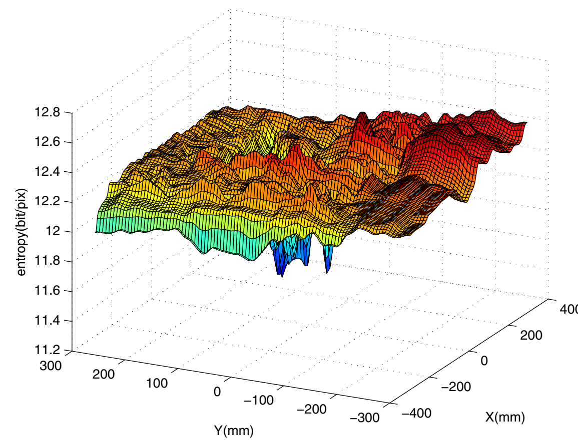

Fig. 4. Entropy Mapping with Multiple Extrema

The second experiment was designed to replicate poor back lighting conditions, in which the camera is partially blinded by a bright light behind a target of interest. This is similar to the images of the cat in Fig. 2. For this experiment, a picture was placed on an easel in front of the robot. A projector was placed behind the easel and slightly to one side. The resulting mapping is shown in Fig. 4. The light from the projector will saturate the camera when they are aligned along the camera optical axis, which gives the clear global minimum of the entropy map. There are many local maximum on the interior. The global maximum corresponds to the camera blocking the light from the projector with the picture on the easel.

B. ESC Design

As shown in [3], there are design variables that affect the stability and performance of ESC systems. These variables include the two dither signals, the high-pass filter, the low-pass filters, and the gain k. The sensors and system plant, i.e. images from a video camera and a robot manipulator, further restrict the choice of design variables. In this initial investigation only two degrees of freedom are used. Hence we need a dither signal of of the form $d_1(t) = [a_1 \sin(\omega_1 t), a_2 \sin(\omega_2 t)]^T$ The choice of frequencies for the dither vector must satisfy the following constraints [3]:

1) $\omega_1 \neq \omega_2$
2) ω_1 and ω_2 are smaller than one half the sampling rate.
3) ω_1 and ω_2 are in the pass band of the high-pass filter and stop band of the low-pass filter.

Video systems generally have frame rate around 30Hz. After the time required for image processing and control calculation, the sampling rate is approximately 20Hz. We employ dither frequencies in the range 5Hz - 9Hz, which can be tuned for performance through trial and error.

The dither signal amplitudes a_1 and a_2 affect the seeking accuracy, convergence speed of the ESC loop. A larger dither amplitude lowers the time for convergence but decreases the accuracy of the final estimate for $\tilde{\theta}$. Designers must also consider the forces necessary to generate dither signals with large amplitudes. For experiments in this paper, considering the speed limit of robot actuators, we chose $a_1 = a_2 = 5cm$.

The cutoff frequency of the high-pass filter should be lower than ω_1 and ω_2. We employ a second order Chebyshev type I filter with a cutoff frequency of 3Hz, given by

$$G_1(z) = \frac{0.5768z^2 - 1.1536z + 0.5768}{z^2 - 1.0900z + 0.4735}. \quad (3)$$

The cutoff frequency of low-pass filter should also be lower than ω_1 and ω_2. We use a second order FIR filter with a cutoff frequency of 1Hz, given by

$$G_2(z) = 0.0680 + 0.8640z^{-1} + 0.0680z^{-2} \quad (4)$$

IV. Simplex Guided Extremum Seeking

As shown in Fig. 4, the entropy function can have multiple local extrema. ESC is very likely to be trapped at a local maximum and can never reach the global global maximum. Therefore, the final result can be heavily affected by initial positions. It has been shown that increasing the amplitude of dither signal can improve the chance to reach the global extremum [27]. However, high amplitude signals can saturate the actuators and make it hard to demodulate the signal to gather the gradient information.

Alternately, a multi-directional algorithm that searches for extrema through the whole workspace, is more likely to find a global maximum [20]–[22]. Multi-directional search algorithms are approaches to linear programming that construct a point simplex and iteratively optimize the point members to converge to the extremum, therefore they are referred to as simplex methods. The maximum point in the simplex is always kept, and a group of linear combinations (reflection, extension, and contraction) are used to predict points with a better value. This continues until the best point is located or a termination condition is met. The downside to simplex methods is poor dynamic response, in that they are not well suited to changing maps, such as the entropy of a changing scene.

Therefore, we propose a combined ES algorithm that can employ simplex methods to search for a global maximum while preserve the dynamic tracking abilities of ESC. We call this method Simplex Guided Extremum Seeking (SGES), which uses a simplex method for large scale searching, and ESC for small-scale local searching. SGES shows strong promise for optimizing other cost functions that have many local extrema that are not global extrema.

For a n dimensional search space, SGES executes ESC at $n+1$ initial trial points to obtain $n+1$ local maxima. The maxima are taken as simplex vertices and denoted as $\mathbf{x}_0^0$, $\mathbf{x}_1^0$, $\mathbf{x}_2^0 ... \mathbf{x}_n^0$. The superscript represents iteration time, and they are ordered after every vertex update, such that $f(\mathbf{x}_0^k) > f(\mathbf{x}_i^k)$ for $i = 1,2...n$ in any kth iteration.

As $\mathbf{x}_0^k$ is the current best maximum, it is reasonable to assume this vertex lies in a more optimal region of the workspace. So we perform reflection to generate n initial trial points $\mathbf{r}_i^k = \mathbf{x}_0^k - \alpha(\mathbf{x}_i^k - \mathbf{x}_0^k)$ for $i = 1,2...n$, where $\alpha > 0$ is a constant. ESC is performed from each trial point, leading to a new group of local maxima, denoted as $\hat{\mathbf{r}}_i^k$.

If there is a local maximum $\hat{\mathbf{r}}_{j_r}^k$, such that $f(\hat{\mathbf{r}}_{j_r}^k) > f(\mathbf{x}_0^k)$ and $0 < j_r \leq n$, it is possible that better points could be found further along this direction. So we perform on extension step, generating n initial trial points $\mathbf{e}_i^k = \mathbf{x}_0^k - \lambda(\mathbf{x}_i^k - \mathbf{x}_0^k)$ for $i = 1,2...n$, where $\lambda > \alpha$ is a constant. ESC is ran from each trial point, producing one more group of maxima $\hat{\mathbf{e}}_i^k$.

If there is a local maximum $\hat{\mathbf{e}}_{j_e}^k$, such that $f(\hat{\mathbf{e}}_{j_e}^k) > f(\hat{\mathbf{r}}_{j_r}^k) > f(\mathbf{x}_0^k)$, and $0 < j_e \leq n$, we accept $\hat{\mathbf{e}}_i^k$ to update the vertices, i.e. $\mathbf{x}_i^{k+1} = \mathbf{e}_i^k$ for $i = 1,2...n$, else we accept $\hat{\mathbf{r}}_i^k$, i.e. $\mathbf{x}_i^{k+1} = \hat{\mathbf{r}}_i^k$ for $i = 1,2...n$.

If there is no $\hat{\mathbf{r}}_{j_r}^k$, such that $f(\hat{\mathbf{r}}_{j_r}^k) > f(\mathbf{x}_0^k)$, we accept the $\mathbf{x}_0^k$ as the current global optimal and contract all $\mathbf{x}_i^k$ for $i = 1,2...n$ towards $\mathbf{x}_0^k$. In this case, generate n initial trial points $\mathbf{c}_i^k = \mathbf{x}_0^k + \theta(\mathbf{x}_i^k - \mathbf{x}_0^k)$, for $i = 1,2...n$, where $0 < \theta < 1$. Again performing ESC from each trial point leads to one more group of local maxima $\hat{\mathbf{c}}_i^k$. If there is some $\hat{\mathbf{c}}_{j_c}^k$, such that $f(\hat{\mathbf{c}}_{j_c}^k) > f(\mathbf{x}_0^k)$, we accept contraction step and update vertices as $\mathbf{x}_i^{k+1} = \hat{\mathbf{c}}_i^k$, for $i = 1,2...n$. Otherwise, we update vertices as $\mathbf{x}_i^{k+1} = \mathbf{c}_i^k$, for $i = 1,2...n$ to guarantee convergence.

Under specific conditions, simplex methods can guarantee convergence of the simplex points set. Given local the stability properties of ESC and global convergence properties of simplex methods, the SGES method should perform well in a variety of problems. Simulations and experiments demonstrate it does work well, outperforming ESC or simplex methods in numerous cases. Future work will attempt to prove that, under specific conditions, SGES will converge to an optimal local maximum and that this optimum will be the maximum point visited.

V. Simulation Results

Using the entropy mappings shown in Section III-A, simulations were conducted to demonstrate the performance of both basic ESC and SGES to maximize image entropy. Three points in the workspace are chosen as initial points for each simulations, $[x, y]^T = [78, -18]$, $[-22, 32]$ and $[78, 72]$.

Using the entropy mapping shown in Fig. 3, the results are shown in Fig. 5. The background of the figure is a contour

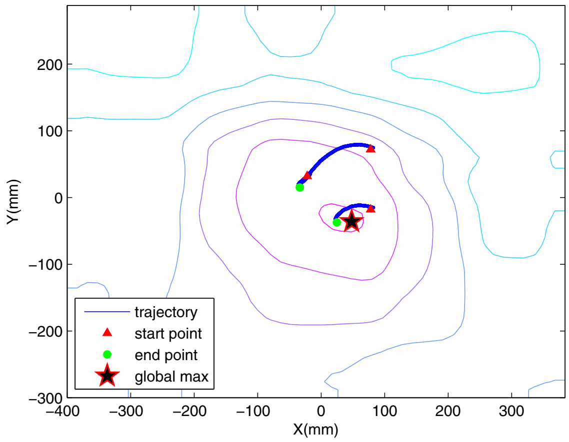

Fig. 5. ESC Simulation on Entropy Mapping I. All initial points converge fairly close to the global maximum.

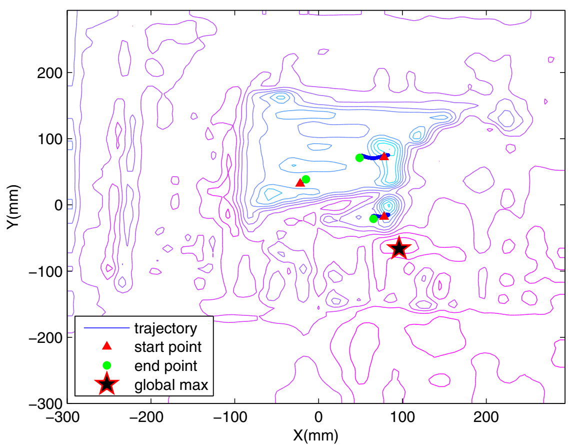

Fig. 6. ESC Simulation on Entropy Mapping II. All initial points converge to local maxima, some quite far from the global maximum.

plot of entropy mapping. The initial point of each trial is denoted as a triangle, and the end points are noted as circles. ESC starting from one of the initial points can converge near the global maximum. This is due to the fact that this mapping has few local maxima. In contrast, when using the mapping in Fig. 4, which has many local maxima, ESC does not converge close to the global maximum. The results are shown in Fig. 6.

SGES is used in a simulation on the map originally shown in Fig. 4. The three initial conditions are used to construct the initial simplex. The SGES algorithm converges very near to the global maximum, as shown in Fig. 7. In Fig. 7, each dash line triangle represents the simplex update step motion.

Fig. 8 is the simplex update plot. The solid line in the top plot indicates the maximum value point in the simplex set, which monotonously increase. The bottom plot indicates the area of the triangle constructed by the three simplex points, which monotonically decreases. This demonstrates the convergence of the SGES in terms of the optimization variables.

The entropy extrema found for each initial condition in each simulation is given in Table I. This indicates that the

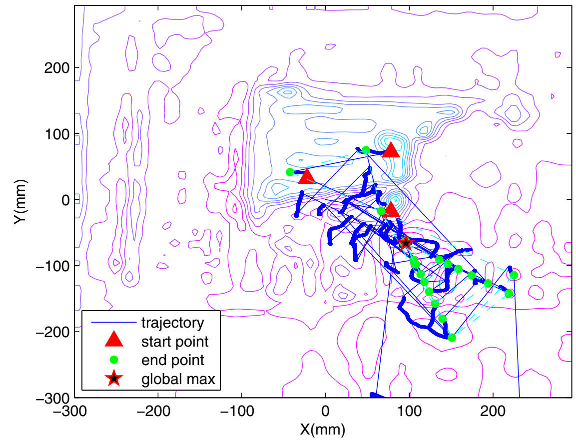

Fig. 7. Simplex Guided ESC Simulation on Entropy Mapping II. The simplex algorithm allows the system to find the global maximum.

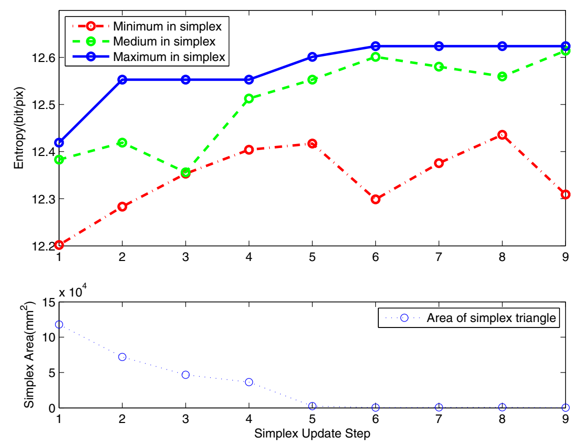

Fig. 8. Simplex Update for SGES Simulation. The simplex points converge in the measure of entropy. At the same time, the area of the polygon the simplex points define gets smaller, indicating they converge in space.

SGES can improve the ability to find converge near the global maximum in terms of the optimization variables and in value of the cost function.

VI. Experiment Results

We conducted experiments to demonstrate the effectiveness of the proposed control method. The ESC scheme is implemented on a six degree of freedom Staubli TX90 robot arm with a camera mounted on the end effector. Two degrees of freedom are used, translation in the $x-y$ plane.

The ESC experiment is implemented for the first scene described in Section III-A, a monochrome poster board with a picture fixed near the center. The result is shown in Fig.

Sim. #	Extremum H achieved	Global Max. H
1	10.48, 10.48, 10.52	10.54
2	12.07, 11.88, 11.87	12.59
3	12.59, 12.59, 12.59	12.59

TABLE I

Entropy extrema found in simulation of the different algorithms

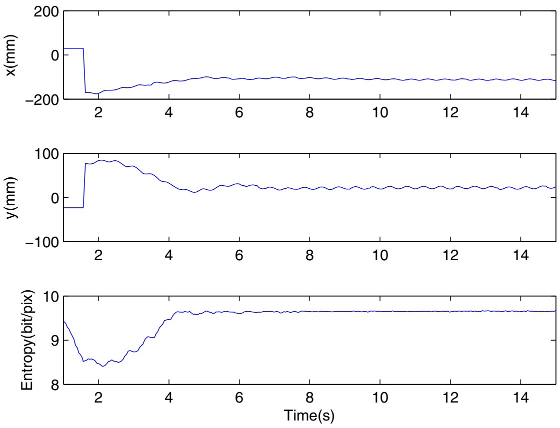

Fig. 9. ESC Experiment results for single maxima scenario

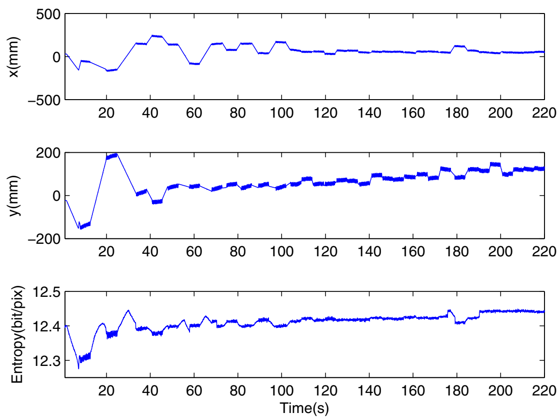

Fig. 10. Experiment result of SGES looking in an empty lab.

9. In this experiment, the camera was placed at an initial position away from the global maximum, and the ESC algorithm quickly guides the camera towards the maximum entropy position, bringing the picture into full view.

An experiment of the SGES system is first implemented for the common scene of our lab. This entropy map is rather flat and has multiple local maximum. We start SGES with three random simplex points. At each point, ESC is employed to find the local maximum. When the system has detected a gradient less than 1.0 for 2 seconds, the system moves to the next predicted simplex point. This switch condition can be tuned for desired performance. The position of the camera and entropy measure over time is shown in Fig. 10. The periods when ESC is operating are identifiable by the periodic dither. The relative straight periods are the times when the system is moving to a new simplex predicted point. Without the simplex process, the system would have settled at the first end point of the ESC section. However, with the simplex, the system does find a higher entropy measure. The simplex update plot is shown in Fig. 11.

The simplex step of SGES improves the global extremum seeking properties. However, without ESC, the system can not respond to a dynamic, changing scene after settling. The following experiment shows the dynamic property of SGES. We conduct this experiment in the second scene described in Section III-A, a picture is placed on an easel with a bright light behind it which can partially blind the camera. This

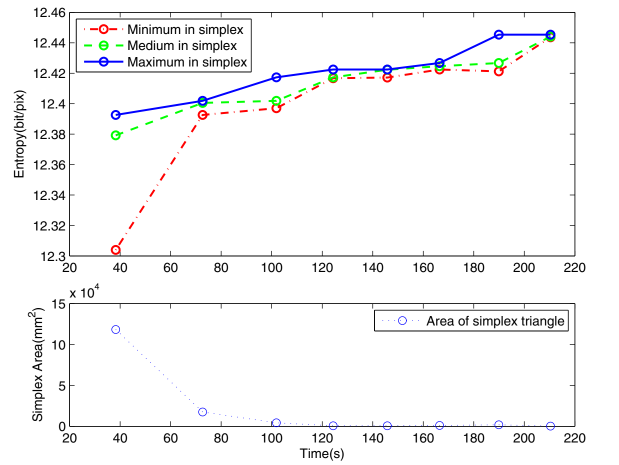

Fig. 11. Simplex Update for SGES Experiment. The simplex vertices converge in terms of entropy value. As the area of the polygon defined by vertices becomes smaller, the location of them converges.

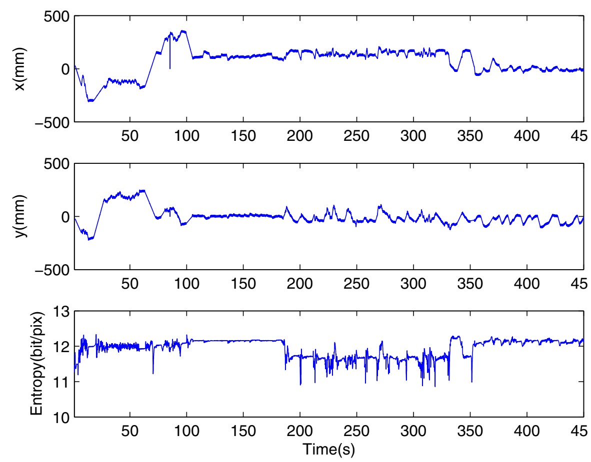

Fig. 12. Experiment of SGES looking at a picture backlight with a bright light. The simplex algorithm allows the system to converge, which entails block out the light. After convergence, the picture is moved. The ESC algorithm alters the simplex points and allows for a second convergence.

can be seen in Fig. 14. The system does converge near the global maximum, which places the picture in front of the blinding light. After the system has been settled for about 80 seconds, the picture was moved to change the scene. As illustrated in Fig. 12, SGES reaches a second convergence point, again blocking the light with the picture. The simplex points are shown in Fig. 13. Several corresponding images are collected in Fig. 14.

VII. Conclusions and Future Work

We have presented an approach to use extremum seeking control to maximize the entropy of a sensor signal. Focusing on mobile cameras, a robot can guide the camera to capture image with maximum entropy. This can focus attention on objects on interest and correct common imaging problems, such as poor lighting conditions. Since entropy maps often have local maxima, we presented a novel approach that combines the global properties of simplex optimization methods and dynamic properties of extremum seeking control.

Experimental validation of the approach shows strong potential. However, this is an initial investigation, and there

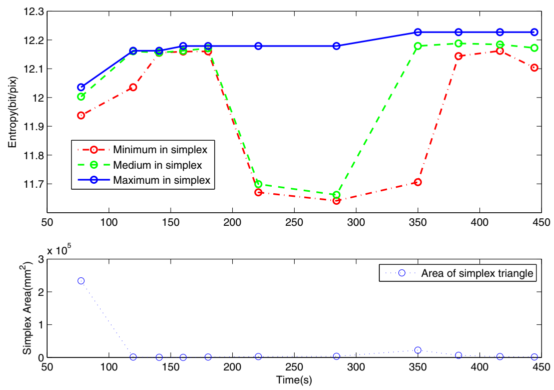

Fig. 13. Simplex Update for the dynamic SGES Experiment. While the entropy measures do not converge as closely in the second convergence, it can be seen that they are very close in space.

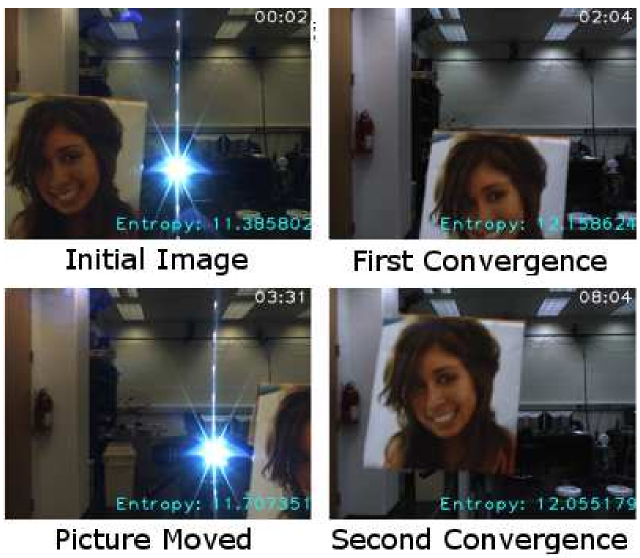

Fig. 14. Critical Scenes for Dynamic SGES Experiment. The backlight can be seem to partially blind the camera in the initial images, and maximization of entropy causes the camera to block the light source.

are many area of future work. Firstly, a formal analysis must be done to prove stability and convergence of the SGES approach. Additionally, this approach may not be well suited for some entropy maps, such as an extremum on the boundary of the workspace, which violates the conditions for ESC and simplex methods. A modified approach may address this. Adding degrees of freedom is an important step. Ultimately, we hope to implement this on mobile robots, requiring consideration of their unique velocity constraints and incorporating obstacle avoidance.

References

[1] J. Sternby, "Extremum control systems: An area for adaptive control," in *Preprints of the Joint American Control Conference*, 1980.

[2] M. Krstic and H.-H. Wang, "Design and stability analysis of extremum seeking feedback for general nonlinear systems," *Proc. Conf. Desision and Control*, pp. 1743–1748, Dec. 1997.

[3] M. A. Rotea, "Analysis of multivariable extremum seeking algorithms," *Proc. American control Conf.*, pp. 433–437, June 2000.

[4] Y. Tan, D. Nesic, I. Mareels, and A. Astolfi, "On global extremum seeking in the presence of local extrema," *Automatica*, vol. 45, Jan. 2009.

[5] C. Shannon and W. Weaver, *The Mathematical Theory of Communication*. Univ of Illinois Press, 1998.

[6] K. Sayood, *Introduction to data compression*. Morgan Kaufmann, 2000.

[7] H. Akaike, *Selected Papers of Hirotugu Akaike*. Springer, 1997.

[8] E. T. Jaynes, "On the rationale of maximum-entropy methods," *Proceedings of the IEEE*, vol. 70, pp. 939–952, 1982.

[9] G. Beni and S. Hackwood, *Toward a Practice of Autonomous Systems*, ch. The maximum entropy principle and sensing in swarm intelligence, pp. 153–159. MIT Press, 1992.

[10] B. R. Abidi, "Automatic sensor placement," in *Intelligent Robots and Computer Vision XIV: Algorithms, Techniques, Active Vision, and Materials Handling* (D. P. Casasent, ed.), vol. 2588, pp. 387–398, 1995.

[11] A. Howard, M. J. Mataric, and G. S. Sukhatme, "Mobile sensor network deployment using potential field: A distributed scalable solution to the area coverage problem," in *Proc. International Conference on Distributed Autonomous Robotic Systems*, pp. 299–308, 2002.

[12] A. T. Murray, K. Kim, J. W. Davis, R. Machiraju, and R. Parent, "Coverage optimization to support security monitoring," *Computers, Environment and Urban Systems*, vol. 31, no. 2, pp. 133 – 147, 2007.

[13] Y. Zou and K. Chakrabarty, "Sensor deployment and target localization in distributed sensor networks," *ACM Trans. Embed. Comput. Syst.*, vol. 3, no. 1, pp. 61–91, 2004.

[14] A. Mittal and L. S. Davis, "A general method for sensor planning in multi-sensor systems: Extension to random occlusion," *International Journal of Computer Vision*, vol. 76, no. 1, pp. 31–52, 2008.

[15] J. Zhao, S.-C. Cheung, and T. Nguyen, "Optimal camera network configurations for visual tagging," *IEEE Journal Selected Topics in Signal Processing*, vol. 2, pp. 464–479, Aug. 2008.

[16] D. Fehr, L. Fiore, and N. Papanikolopoulos, "Issues and solutions in surveillance camera placement," in *Proc. IEEE Conf. Intelligent Robots and Systems*, pp. 3780–3785, 2009.

[17] R. Bodor, A. Drenner, P. Schrater, and N. Papanikolopoulos, "Optimal camera placement for automated surveillance tasks," *Journal of Intelligent and Robotic Systems*, vol. 50, no. 3, pp. 257–295, 2007.

[18] A. O. Ercan, D. B. Yang, A. E. Gamal, and L. J. Guibas, *Distributed Computing in Sensor Systems*, ch. Optimal Placement and Selection of Camera Network Nodes for Target Localization, pp. 389 – 404. Springer Berlin, 2006.

[19] O. C. Imer and T. Basar, "Optimal estimation with limited measurements," *International Journal of Systems, Control and Communications*, vol. 2, pp. 5 – 29, 2010.

[20] G. Dantzig, *Linear programming and extensions*. Landmarks in Physics and Mathematics, Princeton University Press, 1998.

[21] J. A. Nelder and R. Mead, "A simplex method for function minimization," *Computer Journal*, vol. 7, pp. 308–313, 1965.

[22] V. Torczon, "On the convergence of the multidirectional search algorithm," *SIAM Journal on Optimization*, no. 1, 1991.

[23] H. K. Khalil, *Nonlinear Systems*. New Jersey: Prentice Hall, 3 ed., 2002.

[24] J. A. Sanders, F. Verhulst, and J. A. Murdock, *Averaging Methods in Nonlinear Dynamical Systems*. No. 59 in Applied Mathematical Sciences, Springer, 2007.

[25] C. Shannon, "A mathematical theory of communication," *Bell System Technical Journal,*, vol. 27, pp. 623–656, 1948.

[26] A. Sengur and Y. Guo, "Color texture image segmentation based on neutrosophic set and wavelet transformation," *Computer Vision and Image Understanding*, vol. 115, no. 8, pp. 1134 – 1144, 2011.

[27] Y. Tan, D. Nesic, and I. Mareels, "On non-local stability properties of extremum seeking control," *Automatica*, vol. 42, 2006.